

# Vibrational Spectroscopy of the Microsolvated Phenol Cation: Phenol-Dimethyl Ether

Otto Dopfer, Timothy G. Wright,<sup>†‡</sup> Eric Cordes, and Klaus Müller-Dethlefs\*

Contribution from the Institut für Physikalische und Theoretische Chemie, Technische Universität München, Lichtenbergstrasse 4, D-85747 Garching, Germany

Received January 18, 1994. Revised Manuscript Received April 7, 1994<sup>⊙</sup>

**Abstract:** The hydrogen-bonded 1:1 phenol-dimethyl ether complex is studied in a skimmed supersonic jet. Two-photon, two-color resonance-enhanced multiphoton ionization (1 + 1' REMPI) spectroscopy is used to probe the first excited singlet ( $S_1$ ) state, and the spectra obtained here show that the analysis of a previously recorded laser-induced fluorescence excitation spectrum was partially erroneous. The origin of the  $S_1 \leftarrow S_0$  transition is now identified at 35 893.6  $\text{cm}^{-1}$ ; the intermolecular stretch of the  $S_1$  state is determined (for the first time) as 141  $\text{cm}^{-1}$ ; other inter- and intramolecular vibrational structures are also observed and analyzed. Particular  $S_1$  state vibrational levels are selected and then used as intermediate resonances for the zero-kinetic-energy photoelectron (ZEKE) spectroscopic studies. This technique allows the measurement of the intermolecular modes of the cationic complex. These measurements also allow the first determination of the ionization energy as 62 604  $\pm$  5  $\text{cm}^{-1}$  (7.7620  $\pm$  0.0006 eV). The intermolecular bond in the cation is over 6000  $\text{cm}^{-1}$  more stable than that in the neutral complex. A qualitative interpretation of the chemical bonding changes between this complex and other phenol-containing hydrogen-bonded complexes is presented.

## I. Introduction

The study of intermolecular bonding using the technique of photoelectron spectroscopy has been rather limited due to the poor resolution of the technique: reviews covering both the use of X-ray radiation<sup>1</sup> and ultraviolet radiation<sup>2</sup> have been presented. Recently, attention has been paid to photoelectron spectroscopy (PES) applied to hydrogen-bonded complexes with  $\text{cm}^{-1}$  resolution, sufficient to resolve the intermolecular vibrations excited on ionization from the intermediate  $S_1$  electronic state. In particular, the 1:1 phenol-X complexes have been studied, where X =  $\text{H}_2\text{O}$ ,<sup>3,4</sup>  $\text{CH}_3\text{OH}$ ,<sup>5</sup>  $\text{CH}_3\text{CH}_2\text{OH}$ ,<sup>6</sup> and  $\text{C}_6\text{H}_5\text{OH}$ .<sup>7</sup> For the complexes containing  $\text{CH}_3\text{OH}$  and  $\text{CH}_3\text{CH}_2\text{OH}$ , all six intermolecular modes of the corresponding cationic complex could be extracted from the ZEKE spectra, whereas for phenol- $\text{H}_2\text{O}$  and phenol dimer, only five and two fundamentals could yet be identified, respectively. In the case of the phenol-water complex, the assignment of the vibrational frequencies to particular intermolecular normal coordinates was achieved by recording spectra of deuterated species as well as by comparison with *ab initio* calculations.<sup>8</sup> For each of the 1:1 phenol-X complexes mentioned above, the increase in intermolecular bonding energy upon ionization was derived; this increase is clearly due to the additional charge-dipole interactions present in the cation (compared to the neutral states). The technique used to obtain these high-resolution photoelectron spectra is zero-kinetic-energy photoelectron spectroscopy (com-

monly known as "ZEKE spectroscopy")<sup>9</sup> in combination with resonance-enhanced multiphoton ionization (REMPI). The electrons detected are formed from pulsed-electric-field ionization of Rydberg states<sup>10</sup> that are long-lived in the presence of small electric fields;<sup>11</sup> the technique is sometimes known as the ZEKE-PFI technique (PFI = pulsed-electric-field ionization). For a detailed description of the technique, the reader is referred to the review by Müller-Dethlefs and Schlag and to other recent articles.<sup>12,13</sup>

The phenol-dimethyl ether (phenol-DME) complex was chosen for study for a number of reasons. Firstly, it was wondered if the smaller amount of intermolecular vibrational excitation in the phenol-water ZEKE spectra<sup>3,4</sup> (relative to those of the phenol-methanol complex)<sup>5</sup> may be due to some sort of "symmetry effect". The symmetry of the phenol-water complex is  $C_2$  with the mirror plane containing the phenol ring;<sup>8</sup> the symmetry of the phenol-DME complex may also be expected to be of  $C_2$  symmetry (*vide infra*)—in contrast to the phenol-methanol complex whose symmetry is  $C_1$ . Secondly, the phenol-DME complex finishes a study of the series of complexes phenol-water, phenol-methanol, and phenol-DME, where successive hydrogens on water have been replaced by a methyl group. It was anticipated that the neutral states ( $S_0$  and  $S_1$ ) as well as the cationic ground state would be more strongly bound compared to those of phenol-water and phenol-methanol due to the positive inductive effect of the methyl groups. The latter effect has been seen (for the  $S_0$ ) in an infrared study by Millen and co-workers<sup>14</sup>—a study that also looked at the phenol-dimethyl ether complex. Finally, Abe *et al.*,<sup>15</sup> in a supersonic free jet study, have studied the  $S_1$  state of phenol-DME using laser-induced fluorescence (LIF) spectroscopy. In the interpretation of this spectrum they concluded that two rotational isomers existed, with the respective  $S_1$  origins

<sup>†</sup> Royal Society Postdoctoral Fellow.

<sup>‡</sup> Present address: Laser Spectroscopy Facility, Chemistry Department, The Ohio State University, 120 West 18th Avenue, Columbus, OH 43210.

\* To whom correspondence should be addressed.

⊙ Abstract published in *Advance ACS Abstracts*, May 15, 1994.

(1) Hillier, I. H. In *Molecular Interactions*, Vol. 2; Ratajczak, H., Orville-Thomas, W. J., Eds.; John Wiley and Sons: New York, 1981; p 493.

(2) Rao, C. N. R.; Pradeep, T. *Chem. Soc. Rev.* 1991, 20, 477.

(3) Reiser, G.; Dopfer, O.; Lindner, R.; Henri, G.; Müller-Dethlefs, K.; Schlag, E. W.; Colson, S. D. *Chem. Phys. Lett.* 1991, 181, 1. Dopfer, O.; Reiser, G.; Lindner, R.; Müller-Dethlefs, K. *Ber. Bunsen-Ges. Phys. Chem.* 1992, 96, 1259.

(4) Dopfer, O.; Reiser, G.; Müller-Dethlefs, K.; Schlag, E. W.; Colson, S. D. *J. Chem. Phys.*, in press.

(5) Wright, T. G.; Cordes, E.; Dopfer, O.; Müller-Dethlefs, K. *J. Chem. Soc., Faraday Trans.* 1993, 89, 1609.

(6) Cordes, E.; Dopfer, O.; Wright, T. G.; Müller-Dethlefs, K. *J. Phys. Chem.* 1993, 97, 7471.

(7) Dopfer, O.; Lembach, G.; Wright, T. G.; Müller-Dethlefs, K. *J. Chem. Phys.* 1993, 98, 1933.

(8) Hobza, P.; Burcl, R.; Špirko, V.; Dopfer, O.; Müller-Dethlefs, K.; Schlag, E. W. *J. Chem. Phys.*, in press.

(9) Müller-Dethlefs, K.; Schlag, E. W. *Annu. Rev. Phys. Chem.* 1991, 42, 109.

(10) Reiser, G.; Habenicht, W.; Müller-Dethlefs, K.; Schlag, E. W. *Chem. Phys. Lett.* 1988, 152, 119.

(11) Chupka, W. A. *J. Chem. Phys.* 1993, 98, 4520.

(12) Merkt, F.; Softley, T. P. *Int. Rev. Phys. Chem.* 1993, 12, 205.

(13) Grant, E. R.; White, M. G. *Nature* 1991, 354, 249. Pratt, S. T.; Dehmer, P. M.; Dehmer, J. L.; McCormack, E. F. *Comments At. Mol. Phys.* 1993, 28, 259. Wright, T. G.; Reiser, G. F.; Müller-Dethlefs, K. *Chem. Ber.* 1994, 30 (2), 128.

(14) Hussein, M. A.; Millen, D. J.; Mines, G. W. *J. Chem. Soc., Faraday Trans. 2* 1976, 72, 686.

(15) Abe, H.; Mikami, N.; Ito, M. *J. Phys. Chem.* 1982, 86, 1768.

separated in energy by  $107\text{ cm}^{-1}$ ; it was anticipated that the use of mass-selected REMPI would confirm (or disprove) this hypothesis.

## II. Experimental Section

The experimental setup has been described previously,<sup>16</sup> and the small modifications made for the study of the phenol complexes have been outlined elsewhere.<sup>4-7</sup> Very briefly, phenol (Fluka,  $\geq 99.5\%$  purity) was heated (to temperatures up to  $100\text{ }^\circ\text{C}$ ) in a stainless steel oven. Dimethyl ether (Linde,  $\geq 99.6\%$  purity) was introduced into the oven assembly, to a pressure of *ca.* 0.5 bar. The oven assembly was then isolated from the dimethyl ether lecture bottle and connected to an argon carrier gas line. It is believed that the dimethyl ether dissolves to a large extent in the phenol; it was found that significant signals attributable to the phenol-dimethyl ether complex could be obtained for *ca.* 2 weeks, at a nearly constant level. The mixture of argon (5 bar), phenol, and dimethyl ether was coexpanded through a  $300\text{-}\mu\text{m}$  nozzle, which was connected to a pulsed valve (25 Hz), into vacuum. The resulting supersonic jet was skimmed before entering the ionization chamber. The jet was intersected by the outputs of two dye lasers, synchronously pumped by a XeCl excimer laser. The first dye laser, used to pump the  $S_1 \leftarrow S_0$  transition, contained Coumarin 153 and was frequency-doubled in a KDP crystal; the second dye laser, used for the ionization step, contained the laser dye DMQ. As noted above, the pulsed-field variant<sup>10</sup> of ZEKE spectroscopy was used, which relies on the pulsed-electric-field ionization (PFI) of Rydberg states lying a few wavenumbers below an ionization threshold. These PFI electrons are separated from "prompt" electrons by employing a short delay between the laser pulses and the application of the pulsed electric field: this allows the "prompt" electrons to move away from the ionization volume, owing either to the influence of their kinetic energy or to small offset electric fields in the apparatus. The delayed electric extraction pulse used for this work is applied typically 800–1000 ns after the laser pulses and rises to  $0.7\text{ V/cm}$  in 10 ns. Owing to the spatial separation of the "prompt" electrons and the PFI electrons, a very different time-of-flight is exhibited by each of them, allowing their independent detection by the use of electronic gating of the detected electron signal. Time-of-flight mass spectra were recorded with a transient digitizer (Le Croy TR8828C), connected to a PC by a 6010 controller.

The laser containing Coumarin 153 was calibrated ( $<0.2\text{ cm}^{-1}$ ) by comparison of the absorption spectrum of iodine (recorded simultaneously with the REMPI spectrum) with the published spectrum.<sup>17</sup> The laser containing DMQ was calibrated ( $<1\text{ cm}^{-1}$ ) against the well-known emission lines of neon and mercury. All laser frequencies have been converted from those in air to those in vacuum. The spectra are all uncorrected for dye laser intensity output variations.

## III. Results and Discussion

**A. REMPI Spectroscopy.** The two-photon, two-color ( $1 + 1'$ ) REMPI spectrum of the phenol-DME complex is shown in Figure 1 for a range of internal  $S_1$  energies up to *ca.*  $1000\text{ cm}^{-1}$ . In the region near the  $S_1$  origin (see Figure 2) some low-frequency intermolecular vibrations are visible. At first sight, the interpretation of this spectrum looks clear, with a progression containing components of a low-frequency intermolecular bend, denoted  $\xi_1$ , with separations of *ca.*  $26.5\text{ cm}^{-1}$ . In addition, the intermolecular stretch, denoted  $\sigma$ , is observed with a frequency of  $141.3\text{ cm}^{-1}$ . However, when comparison of the present REMPI spectrum (see Figure 3b,c) is made with the LIF spectrum of Abe

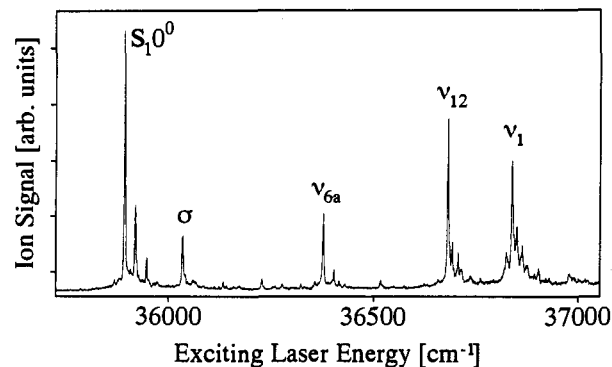


**Figure 1.** ( $1 + 1'$ ) REMPI spectrum of the phenol-dimethyl ether complex: full scan. The intermolecular stretch vibration is marked with  $\sigma$ , while  $\nu_i$  indicate intramolecular phenol-localized vibrations. The ionizing laser was set to 350 nm. See text for details.

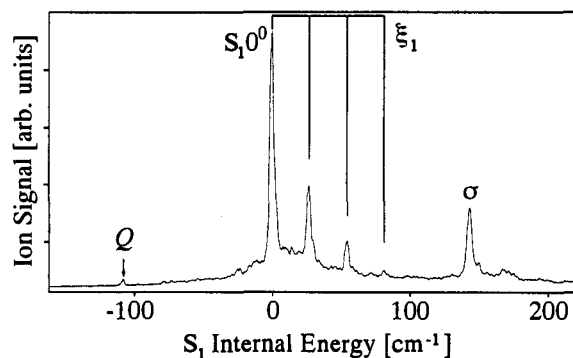


**Figure 2.** ( $1 + 1'$ ) REMPI spectrum of the phenol-dimethyl ether complex: region around the  $S_1$  origin. The comb indicates a progression of an intermolecular bend, denoted  $\xi_1$ . The band indicated with  $Q$  is probably due to a water-containing complex. The ionizing laser was set to 350 nm. See text for details.

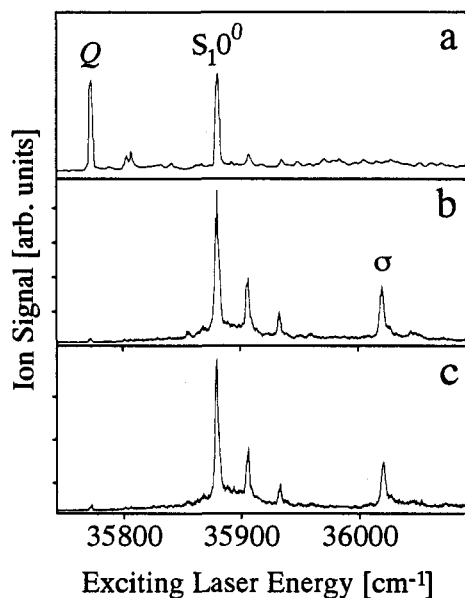


**Figure 3.** Comparison of the LIF spectrum of the phenol-dimethyl ether complex ((a) from ref 15) and the ( $1 + 1'$ ) REMPI spectra obtained in this work ((b) 2 bar of argon and (c) 5 bar of argon as carrier gas pressure). Note that there are different relative intensities in the bands marked with  $Q$  and  $\sigma$ . The band indicated with  $Q$  is probably due to a water-containing complex, while  $\sigma$  indicates the intermolecular stretch of the phenol-DME complex in the  $S_1$  state. For the REMPI spectra, the ionizing laser was set to 350 nm. See text for details.

(16) Habenicht, W.; Reiser, G.; Müller-Dethlefs, K. *J. Chem. Phys.* **1991**, *95*, 4809.

(17) Gerstencorn, S.; Luc, P. *Atlas du Spectra d'Absorption de la Molécule d'Iode*; CNRS: Paris, 1980.

*et al.*<sup>15</sup> (see Figure 3a), then it can be seen that there are some differences between the two different types of spectra obtained. The most obvious discrepancy is in the band marked  $Q$  in Figures

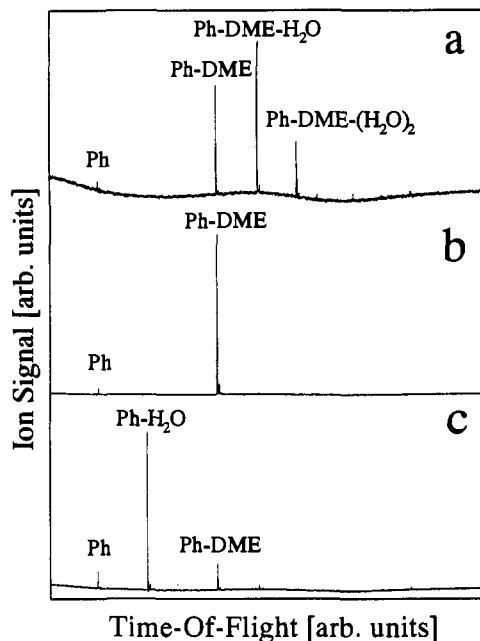


**Figure 4.** Mass spectra recorded at different excitation energies: excitation energy resonant (a) with feature *Q*, (b) with the  $S_1$  origin of phenol-DME, and (c) with the  $S_1$  origin of the phenol-water complex. The ionizing laser was set to 350 nm. See text for details.

2 and 3a. In the LIF work,<sup>15</sup> feature *Q* was assigned to the  $S_1$  origin of one rotational isomer of the 1:1 phenol-dimethyl ether complex, while the  $S_1$  origin band indicated in Figure 2 was assigned to the  $S_1$  origin of another rotational isomer. The astonishing fact is that, in the LIF spectrum, this band appears at the same intensity as the most intense feature in Figure 2, whereas in the  $(1 + 1')$  REMPI spectrum in Figure 2, it is barely visible. This band is not a hot band, since the REMPI spectra recorded using 2 and 5 bar of argon as a backing gas are almost identical (see Figure 3, parts b and c, respectively). Since the LIF technique is not mass specific, in contrast to the REMPI technique used here, a possible explanation is that this feature is due to some other species. (Other plausible explanations would be that, for the two isomers, the fluorescence yield ratio is different from the ionization cross section ratio or, secondly, that the jet conditions are different in the two studies, producing a different isomer ratio; however, such large differences seem unlikely.) In order to ascertain what this species was, the first step was the recording of a mass spectrum of the ions resulting from irradiation with the exciting laser set at two resonances: that of feature *Q* (indicated in Figure 3a) and that of the most intense band in the REMPI spectrum shown in Figure 3b (the results are shown in Figure 4a,b). As may be seen, at a frequency corresponding to the most intense feature in Figure 3b,  $[\text{phenol-DME}]^+$  is the largest feature by far in the mass spectrum (shown in Figure 4b); a small amount of  $\text{phenol}^+$  is also present, resulting from fragmentation of excited  $[\text{phenol-DME}]^+$  ions formed from two-photon, one-color ionization, *i.e.* two photons from the first laser have been absorbed. (The  $\text{phenol}^+$  peak is very weak due to the large fraction—over 90%—of two-photon, two-color soft ionization employed here.) If the frequency of the exciting laser is resonant with feature *Q* (see Figure 3a), then the corresponding mass spectrum (shown in Figure 4a) is rather different:  $[\text{phenol-DME-water}]^+$  and  $[\text{phenol-DME-(water)}_2]^+$  are of intensity greater than, or of intensity comparable to, that of  $[\text{phenol-DME}]^+$ ; again  $\text{phenol}^+$  fragments also appear. The assignment of feature *Q* in the LIF spectrum to a water-containing complex seems clear just from these data, but it is a surprising result since significant precautions were taken in the LIF work to avoid water contamination (*viz.* the phenol was dehydrated and purified by sublimation under vacuum three times and the solvents used were

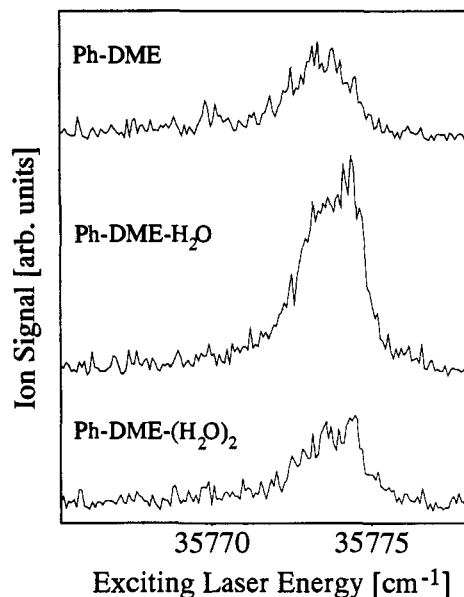


**Figure 5.**  $(1 + 1')$  REMPI spectra scanning over feature *Q* recorded in different mass channels: (top) phenol-DME; (middle) phenol-DME-water; (bottom) phenol-DME-(water)<sub>2</sub>. The ionizing laser was set to 350 nm. See text for details.

of spectroscopic or special grade in that work<sup>15</sup>); no such precautions were taken in this work. In Figure 4c a mass spectrum is shown, with the exciting laser energy set to the phenol-water  $S_1$  origin resonance. As expected, the mass peak corresponding to the phenol-water cation is dominating the time-of-flight spectrum proving again that significant water impurity is present in the reservoir. (It should be noted here that the selectivity at the phenol-DME resonance for the phenol-DME complex in Figure 4b is very high: no water-containing complexes are seen at all in this spectrum.) As further proof that, somehow, some water-containing species did contribute to the LIF spectrum, Figure 5 shows a scan across feature *Q* with time-of-flight gates set for the masses of  $[\text{phenol-DME}]^+$ ,  $[\text{phenol-DME-water}]^+$ , and  $[\text{phenol-DME-(water)}_2]^+$ . Although the intensity in the mass gate of the two-water complex is less than that in the other two mass channels, it is believed that feature *Q* is due to phenol-DME-(water)<sub>2</sub>, or possibly a complex with even more water molecules attached, but that the ions are fragmenting before they reach the detector. This conclusion is further supported by a series of mass spectra recorded with the first laser fixed at the wavelength of feature *Q* and with the second laser fixed on different wavelengths that are lower and lower in energy (the results are shown in Figure 6). As the photon energy of the ionizing laser decreases, so do the relative intensities of the mass peaks corresponding to the water-containing complexes. The lower the energy of the second laser, the lower the cross section for ionization with the second color; hence, the proportion of the one-color multiphoton ionization increases resulting in a higher fragmentation rate of phenol-DME-(water)<sub>n</sub> into phenol-DME-(water)<sub>n-1</sub> cations. At a wavelength of 375 nm, the ionization energy of phenol-DME is not reached (*vide infra*) and so all the  $[\text{phenol-DME}]^+$  signal here must arise from one-color ionization by absorption of two photons from the first laser and/or fragmentation of some water-containing phenol-DME complexes. These mass spectra indicate again that feature *Q* arises from a phenol-DME-(water)<sub>n</sub> species, probably with  $n = 2$ . Hence, the most intense peak in Figure 2 is assigned as the origin of the  $S_1 \leftarrow S_0$  transition for the phenol-DME complex; its position was determined as 35 893.6  $\text{cm}^{-1}$ , in good agreement with the previous study<sup>15</sup> (where this particular band, however, was assigned to the  $S_1$  origin of a *second* isomer). This represents a red shift of 455

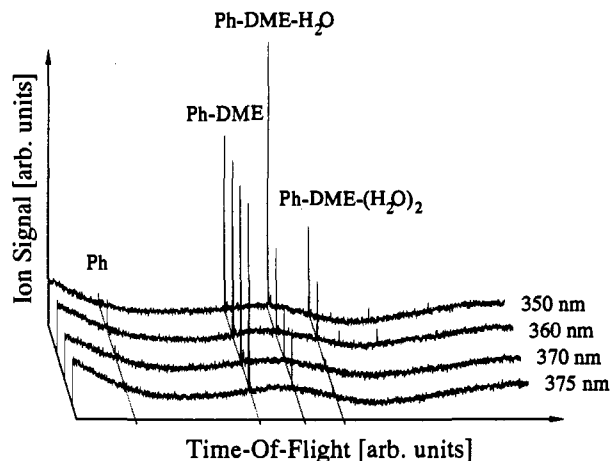


Figure 6. Mass spectra recorded with the exciting laser fixed at the energy of feature  $Q$ ; different values of the ionization laser wavelength have been used. The spectra are individually normalized to the intensity of the phenol-DME peak. See text for details.

$\text{cm}^{-1}$  relative to the origin of the  $S_1 \leftarrow S_0$  transition in phenol (which is situated at  $36\,348.7\text{ cm}^{-1}$ ).<sup>18</sup>

A further discrepancy between the LIF and the REMPI spectra (see Figure 3a,b) is the intensity of the intermolecular stretch ( $\sigma$ ) band. In contrast to the LIF spectrum where this band is almost quenched in intensity, the band can clearly be seen in the REMPI spectrum and its frequency could be determined in the present work for the first time as  $141\text{ cm}^{-1}$ . The assignment of this band to the phenol-DME complex seems clear, since in the REMPI spectrum the low-frequency bend progression is observed in combination with this band (although these combination bands are less intense) and also a weak feature at  $280\text{ cm}^{-1}$  is found which can be assigned to the first overtone. The assignment of this band to the intermolecular stretch is justified by the expected frequency value from comparison with other similar phenol-containing 1:1 complexes.<sup>4,5,6,7,15,19,20</sup> The difference in the intensity of the stretch band in the LIF and REMPI spectra is not completely clear but may be due to a reduced fluorescence yield due to rapid intramolecular vibrational redistribution. The interpretation of the low-energy region of the REMPI spectrum in terms of a low-frequency bending progression of  $\xi_1$  and the intermolecular stretch seems to be established.

To the red side of the  $S_1$  origin, small features attributed to hot bands can be seen. The most intense feature is *ca.*  $24\text{ cm}^{-1}$  red-shifted and is probably due to the  $S_1 \leftarrow S_0\ \xi_{11}^0$  transition, giving a ground-state bending frequency of  $24\text{ cm}^{-1}$ . No ground-state frequencies are known for the phenol-dimethyl ether complex (for example, from dispersed LIF spectra), but the frequency value of  $24\text{ cm}^{-1}$  for an intermolecular bend is consistent with data available for other similar hydrogen-bonded phenol complexes.<sup>19,20</sup>

As may be seen from Figure 1, there are also a number of intense intramolecular (phenol-localized) vibrations—labeled  $\nu_i$ —which are assigned by comparison with the UV absorption spectra of phenol by Bist *et al.*<sup>21</sup> They exhibit small shifts due to complexation, and these are presented in Table 1. As may be seen by comparison with previous determinations of intramolecular phenol-localized vibrations, the complexation shifts are qualitatively similar for all of these complexes.<sup>4-7</sup> These intramolecular vibrations demonstrate combination bands with the intermolecular vibrations, showing a similar pattern to that on the  $S_1$  origin. There are also a number of other weak features in the REMPI

Table 1. Frequencies<sup>a</sup> and Complexation Shifts ( $\text{cm}^{-1}$ ) of Phenol-Localized Intramolecular Vibrations ( $S_1$  State)

	$\nu_{6a}$	$\nu_{12}$	$\nu_1$
phenol	476	783	935
phenol-DME	484	787	944
shift <sup>b</sup>	+8	+4	+9

<sup>a</sup> The values are accurate to  $\pm 1\text{ cm}^{-1}$ . <sup>b</sup> Shift = (value in complex - value in monomer).

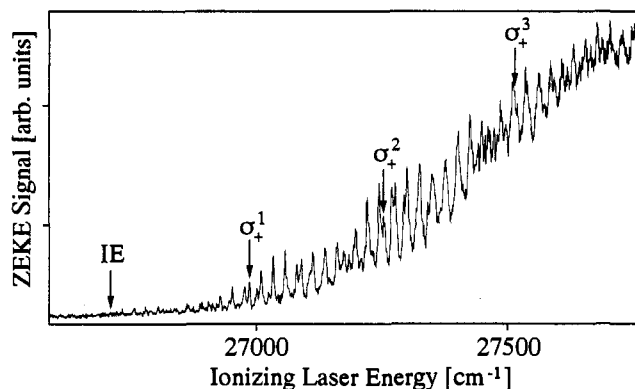


Figure 7. ZEKE spectrum of the phenol-dimethyl ether complex recorded *via* the  $S_1\ 0^0$  level as an intermediate resonance: full scan. IE indicates the ionization energy, while  $\sigma_+^n$  indicates the intermolecular stretch progression of the ionic complex. See text for details.

spectrum which show at least 1 quantum of the intermolecular bending mode superimposed. These are attributed to further intramolecular phenol-localized vibrations, and the values (not listed in Table 1) and also the assignments (if known) are given for completeness:  $240, 335, 366$  (possibly  $\nu_4$ ),  $383, 430, 523$  ( $\nu_{6b}$ ),  $931, 956, 1009\text{ cm}^{-1}$ . In addition, intramolecular phenol-localized vibrations are also found for feature  $Q$ , namely the  $\nu_{6a}$ , the  $\nu_{12}$ , and the  $\nu_1$ . The relative intensities of the latter  $Q$ -related peaks (compared to the phenol-DME features) did decrease over a number of days from the time the reservoir was filled, and this provides some additional proof that they originate from water-containing complexes.

**B. ZEKE Spectroscopy.** ZEKE spectra were recorded from five intermediate  $S_1$  vibronic states: the origin (vibrationless level), the intermolecular vibrational  $\xi_1, \xi_1^2$ , and  $\sigma$  levels, and the intramolecular  $\nu_{6a}$  level.

**ZEKE Spectrum via the  $S_1\ 0^0$  Level.** The ZEKE spectrum obtained *via* the vibrationless level of the  $S_1$  state is shown in Figure 7. As may be seen, it consists of much vibrational structure on a rising "background". This background has also been seen in previous ZEKE studies of similar phenol-containing complexes<sup>5-7</sup> and is probably due to congested vibrational structure, owing to overtones and combinations of the six intermolecular modes with each other, and additionally, to higher energies, with the intramolecular, phenol-localized vibrations (some of which were identified in the studies on phenol-water<sup>4</sup> and phenol-ethanol<sup>6</sup>). The interpretation, owing to the overlapping nature of the different combination series, is not facile, but it is believed that a consistent assignment has been found. In Figure 7, the pure intermolecular stretch progression ( $\sigma_+^n$ ) is noted. The other intermolecular modes are indicated in Figure 8, showing a spectrum recorded (with a better signal-to-noise ratio due to an average over more laser shots per data point) in the vicinity of the ionization energy. The adiabatic ionization energy is taken as the position of the lowest-energy band in the ZEKE spectrum and is indicated in Figure 8. Several scans with averages ranging from 50 to 400 shots per data point were made over the ionization energy region, and no reproducible feature could be observed below the IE band indicated in Figure 8, suggesting that the true ionization energy has been found. (However, it cannot be completely ruled out that the adiabatic ionization energy is in

(18) Martinez, S. J., III; Alfano, J. C.; Levy, D. H. *J. Mol. Spectrosc.* **1992**, *152*, 80.

(19) Ito, M. *J. Mol. Struct.* **1988**, *177*, 173.

(20) Abe, H.; Mikami, N.; Ito, M. *J. Phys. Chem.* **1982**, *86*, 2567.

(21) Bist, H. D.; Brand, J. C. D.; Williams, D. R. *J. Mol. Spectrosc.* **1967**, *24*, 402.

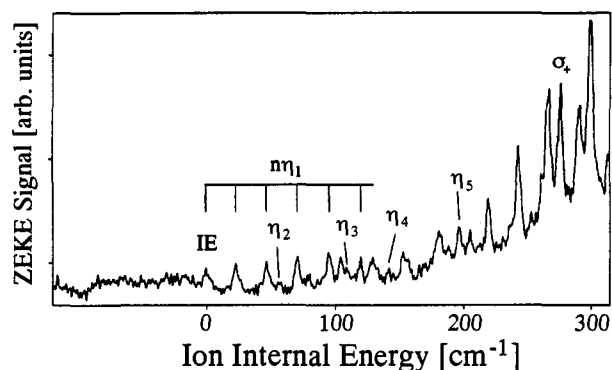


**Figure 8.** ZEKE spectrum of the phenol–dimethyl ether complex recorded *via* the  $S_1$   $0^0$  level as an intermediate resonance. In this spectrum the signal-to-noise ratio is improved due to a higher averaging rate (100 laser shots per data point) compared to that for the spectrum shown in Figure 7. The comb indicates the progression of an intermolecular bend vibration, denoted  $\eta_1$ , starting on the ionization energy band (IE). Further  $\eta_1$  progressions in combination with other intermolecular vibrational fundamentals of the ionic complex (which are denoted  $\eta_i$ ,  $i = 2-5$ , for other bends and the torsion, and  $\sigma_+$  for the stretch) are observed, but these are not indicated in the figure in order to avoid congestion. See text for details.

**Table 2.** Intermolecular Vibrational Frequencies of the Phenol–Dimethyl Ether Cation

vibrational mode <sup>a</sup>	frequency [cm <sup>-1</sup> ] <sup>b</sup>	vibrational mode <sup>a</sup>	frequency [cm <sup>-1</sup> ] <sup>b</sup>
$\eta_1$	24	$\eta_4$	[141] <sup>c</sup>
$\eta_2$	57	$\eta_5$	196
$\eta_3$	109	$\sigma_+$	275

<sup>a</sup>  $\eta_i$  are intermolecular bends or the torsion. <sup>b</sup> The values are accurate to  $\pm 1$  cm<sup>-1</sup>. <sup>c</sup> Tentative assignment.

fact even lower than the value given here because of the very poor Franck–Condon factors near the ionization threshold.) The adiabatic ionization energy is thus determined as  $62\,601 \pm 5$  cm<sup>-1</sup>, with the error arising from the error in laser calibration, plus the width of the ZEKE band at the threshold. This value must be corrected for the ionization energy lowering effect of the pulsed electric field,  $F$ , and a value of 3 cm<sup>-1</sup> is used, consistent with previous work<sup>4-7</sup> and also in line with the accurate determination of the offset field in the present apparatus.<sup>10</sup> This value is also close to the  $4\sqrt{F}$  cm<sup>-1</sup> shift ( $F$  in V/cm) discussed in the work of Chupka.<sup>11</sup> Thus, finally, a field-free adiabatic ionization energy of  $62\,604 \pm 5$  cm<sup>-1</sup> is obtained; this represents a decrease in ionization energy over that of phenol ( $68\,628 \pm 5$  cm<sup>-1</sup>)<sup>22</sup> of  $6024 \pm 10$  cm<sup>-1</sup>.

Figure 8 shows the assignment of the intermolecular vibrational structure of the phenol–DME cation near to the adiabatic ionization threshold. The prominent features are progressions of at least 4 quanta of a low-frequency intermolecular bending mode of 24 cm<sup>-1</sup>, denoted  $\eta_1$  ( $\eta_i$ ,  $i = 1-5$ , is used here for the different intermolecular bending modes as well as for the intermolecular torsion, since they are not differentiable with the present results). This progression is observed on its own (*i.e.* on the IE band, see the comb in Figure 8) as well as in combination with other intermolecular vibrational origins, namely  $\eta_2$  (57 cm<sup>-1</sup>),  $\eta_3$  (109 cm<sup>-1</sup>),  $\eta_4$  (141 cm<sup>-1</sup>),  $\eta_5$  (196 cm<sup>-1</sup>), and  $\sigma_+$  (275 cm<sup>-1</sup>). The measured frequencies are also summarized in Table 2. The assignment is reasonably certain, except for the 141-cm<sup>-1</sup> vibration (denoted  $\eta_4$ ), which is a tentative assignment. The  $\eta_1$  progression on the  $\eta_4$  origin (including the  $\eta_4$  band) may belong to the pure  $\eta_1$  progression; however, there would then be a sudden jump in the frequency of the  $\eta_1$  components to higher frequency at the  $\eta_4$  position. Hence, the assignment of the 141-cm<sup>-1</sup> band to a new intermolecular fundamental  $\eta_4$  is favored here. However,

(22) Lembach, G.; *et al.* To be submitted.

**Table 3.** Intermolecular Vibrational Frequencies of Different Phenol–X Cations

X	observed intermolecular frequencies <sup>a</sup> [cm <sup>-1</sup> ]
H <sub>2</sub> O <sup>b</sup>	67, 84, <b>240</b> , 257, <sup>c</sup> 328
CH <sub>3</sub> OH <sup>d</sup>	34, 52, 76, 153, 158, <b>278</b>
CH <sub>3</sub> CH <sub>2</sub> OH <sup>e</sup>	25, 38, 53, 107, 248, <b>279</b>
C <sub>6</sub> H <sub>5</sub> OH <sup>f</sup>	19, <b>181</b>

<sup>a</sup> Numbers in bold italic correspond to the intermolecular stretch for each complex. <sup>b</sup> From ref 4. <sup>c</sup> Assigned to the first overtone of the intermolecular torsion (for details see ref 4). <sup>d</sup> From ref 5. <sup>e</sup> From ref 6. <sup>f</sup> From ref 7.

**Table 4.** Ionization Energies (IE) and Respective Complexation Shifts ( $\Delta$ IE) of Phenol–X Complexes<sup>a</sup>

species	IE <sup>b</sup>	$\Delta$ IE <sup>c</sup>	$\Delta S_1$ <sup>d</sup>
phenol <sup>e</sup>	68 628	0	0
phenol–H <sub>2</sub> O <sup>f</sup>	64 027	4 601	353
phenol–CH <sub>3</sub> OH <sup>g</sup>	63 207	5 421	416
phenol–CH <sub>3</sub> OCH <sub>3</sub>	62 604	6 024	455
phenol–C <sub>2</sub> H <sub>5</sub> OH <sup>h</sup>	62 901	5 727	410
phenol–phenol <sup>i</sup>	63 649	4 980	305

<sup>a</sup> For comparison, the complexation shifts of the corresponding  $S_1$  origins ( $\Delta S_1$ ) are also presented. All values are given in cm<sup>-1</sup>. <sup>b</sup> The values are corrected for the pulsed extraction field and are accurate to ca.  $\pm 5$  cm<sup>-1</sup>. <sup>c</sup> Where  $\Delta$ IE = IE(phenol) – IE(phenol–X). The values are accurate to ca.  $\pm 10$  cm<sup>-1</sup>. <sup>d</sup> Where  $\Delta S_1$  = (energy of  $S_1$  ←  $S_0$  origin of phenol) – (energy of  $S_1$  ←  $S_0$  origin of phenol–X). The values are accurate to  $\pm 1$  cm<sup>-1</sup>. <sup>e</sup> From ref 22. <sup>f</sup> From ref 4. <sup>g</sup> From ref 5. <sup>h</sup> From ref 6. <sup>i</sup> From ref 7. The values are given for the proton-donating phenol molecule.

a definitive decision is difficult, since the intensities of the relevant bands are low. The stretch frequency of 275 cm<sup>-1</sup> is a large increase over that in the  $S_1$  state (141 cm<sup>-1</sup>), and this, together with the large lowering of ionization energy, reflects the effect of the additional charge–dipole interaction present in the cation. For comparison, the frequencies of the cations of the other studied complexes are given in Table 3. As noted previously,<sup>23</sup> the correlation of the intermolecular modes between the different complexes studied is far from easy, and this is attributed to the subtle bonding, steric and reduced mass effects, and different hydrogen-bond strengths in the complexes. Note, for example, that DME and ethanol have the same molecular mass and that the ionic stretch frequencies are very similar (see Tables 2 and 3) despite the significant difference in binding energy (inferred from Table 4).

Nearly all bands observed in the long ZEKE spectrum *via* the  $S_1$  origin (shown in Figure 7) can be explained by overtone and combination bands of the six intermolecular modes (mainly including  $\eta_1$  and  $\sigma_+$  progressions). The only evidence for an intramolecular phenol-localized mode is found at 464 cm<sup>-1</sup>, which can be assigned to the 18b vibration by comparison with the corresponding frequencies in phenol–water<sup>4</sup> (450 cm<sup>-1</sup>) and phenol–ethanol<sup>6</sup> (465 cm<sup>-1</sup>). Other intramolecular phenol-localized vibrations could not be identified; however, they may be hidden in the rising background or behind the dense intermolecular structure, making their observation difficult. Finally, it is noted that, for the lowest vibration in the DME monomer, namely the symmetric in-phase torsion of the methyl groups, a frequency of 199 cm<sup>-1</sup> has been measured.<sup>24,25</sup> This frequency value is close to the  $\eta_5$  frequency of 196 cm<sup>-1</sup>. However, as mentioned above, an assignment of this vibrational origin to an intermolecular fundamental of the ionic complex is favored here, since the electronic excitation is localized on the phenol

(23) Dopfer, O.; Wright, T. G.; Müller-Dethlefs, K. *J. Electron Spectrosc. Relat. Phenom.*, in press.

(24) Groner, P.; Durig, J. R. *J. Chem. Phys.* 1977, 66, 1856.

(25) Dasgupta, S.; Smith, K. A.; Goddard, W. A., III. *J. Phys. Chem.* 1993, 97, 10891.

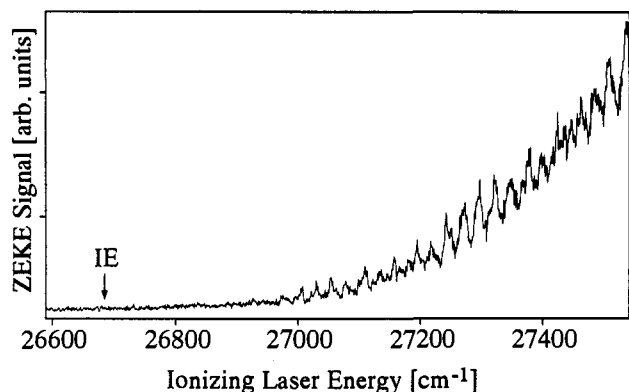


Figure 9. ZEKE spectrum of the phenol-dimethyl ether complex recorded via the  $S_1 \xi_1$  level as an intermediate resonance. The ionization energy (IE) determined from the other spectra is indicated by an arrow.

moiety and, hence, DME-localized intramolecular vibrations are not expected to be excited.

**ZEKE Spectrum via the Intermolecular Vibrational  $S_1 \xi_1$  Level.** The ZEKE spectrum obtained when exciting through the  $S_1$  state with 1 quantum of the  $\xi_1$  vibration excited is shown in Figure 9. As may be seen, the threshold is very much weaker than in the ZEKE spectrum via the  $S_1$  origin. This is due, in part, to the weaker transition into the  $S_1$  state (see Figure 2) but may also be due to poorer Franck-Condon factors for the ionization step from this intermediate state. The analysis of this spectrum supports the assignments given above; the vibrational structure in this spectrum is all interpretable in terms of the inter- and intramolecular modes already determined from the ZEKE spectrum exciting via the  $S_1 0^0$  level.

**ZEKE Spectra via the Intermolecular  $S_1 \xi_1^2$  and  $S_1 \sigma$  and the Intramolecular  $S_1 \nu_{6a}$  Levels.** ZEKE spectra were also recorded when exciting through the  $S_1$  state with 2 quanta of the intermolecular  $\xi_1$  vibration excited or with 1 quantum of the intermolecular stretch excited. The spectrum from the former level did show some vibrational structure, but the signal-to-noise ratio was poor (attributed to the weak  $S_1 \leftarrow S_0$  transition) and no new information was gained from this spectrum. When the stretch was excited in the  $S_1$  state, the ZEKE spectrum was structureless, and the same result has been found for the ZEKE spectrum via the intramolecular  $S_1 \nu_{6a}$  level. This effect had been seen earlier in the cases of the phenol dimer<sup>7</sup> and the phenol-ethanol<sup>6</sup> complexes; interestingly, well-structured ZEKE spectra were obtained for the phenol-water<sup>4</sup> and phenol-methanol<sup>5</sup> complexes, when exciting through the respective  $S_1 \sigma$  levels. For phenol-water, structured ZEKE spectra were found even when the intramolecular  $\nu_{6a}$  or the  $\nu_{12}$  was excited in the  $S_1$  state.<sup>26</sup> The structureless spectra were attributed to fast intracomplex vibrational redistribution (IVR) in the  $S_1$  state. As a trend, it is found that the bigger the solvent molecule becomes (*i.e.* the lower the frequency of the intermolecular vibrations and hence the higher the state density at a given excess energy in the  $S_1$  state) the lower the vibrational excitation energies in the intermediate state that are needed before structureless ZEKE spectra occur. IVR in these complexes and the effect on the obtained ZEKE spectra have been discussed in detail previously<sup>5</sup> and so will not be commented on further here. IVR may also be the reason for the low intensity of the intermolecular stretch band in the LIF spectrum of the  $S_1$  state (compared to the corresponding REMPI spectrum; see Figure 3a,b).

#### IV. Further Discussion

**A. The Hydrogen-Bond Strength.** The decrease in the ionization energy of the phenol-DME complex, with respect to

that of the phenol monomer, of 6024  $\text{cm}^{-1}$  represents the largest decrease of all the phenol complexes studied so far in this laboratory and, hence, implies the strongest intermolecular bond (although the actual value of the bond strength in the neutral will have some effect). The decreases for the phenol-X series for X =  $\text{H}_2\text{O}$ ,  $\text{CH}_3\text{OH}$ , and  $\text{CH}_3\text{OCH}_3$  are 4601, 5421, and 6024  $\text{cm}^{-1}$  (refer to Table 4). This decrease can be ascribed to the well-known +I (positive inductive) effect of the methyl group. The substitution of the first hydrogen on water with a methyl group gives an added decrease of 820  $\text{cm}^{-1}$  in ionization energy over that for phenol- $\text{H}_2\text{O}$ , while the additional substitution of the second hydrogen gives an additional effect of 603  $\text{cm}^{-1}$ . The decrease due to electronic effects will also be modified slightly by steric effects, although these should be rather small for a methyl group. The hydrogen bond increases in strength since the +I effect effectively makes the lone pair on the oxygen atom of the non-phenol moiety more available, so that it can bind more effectively to the acidic proton of the phenol; *i.e.* the methyl groups are making the proton-accepting oxygens more basic. This effect of the methyl group (Me) is well-known. For example, for the series of compounds  $\text{BuNH}_2$ ,  $\text{Bu}_2\text{NH}$ , and  $\text{Bu}_3\text{N}$ , the basicity, in chlorobenzene solvent, increases as the number of butyl groups (Bu) increases; the same general result has been inferred for gas-phase complexes involving  $\text{NH}_3$ ,  $\text{MeNH}_2$ ,  $\text{Me}_2\text{NH}$ , and  $\text{Me}_3\text{N}$  bonded to trichloromethane (chloroform).<sup>27</sup> *In general, this ordering only occurs when hydrogen bonding to the solvent cannot occur* (as is the case here—there being no additional solvent in the vacuum); if hydrogen bonding can occur (*e.g.* in solution in water), then the order of basicity changes to  $\text{Bu}_3\text{N} < \text{BuNH}_2 < \text{Bu}_2\text{NH}$  due to the balance between the availability of the nitrogen lone pair and the possibilities of hydrogen bonding to the solvent through the N-H hydrogens.<sup>28</sup> This is a good example of the difference between the liquid-phase basicity/acidity and the gas-phase basicity/acidity.

It is also possible to look at another series, namely phenol-Y for Y =  $\text{H}_2\text{O}$ ,  $\text{CH}_3\text{OH}$ , and  $\text{CH}_3\text{CH}_2\text{OH}$ ; here the lowerings in ionization energy are 4601, 5421, and 5727  $\text{cm}^{-1}$  (see also Table 4). Note the large difference between water and methanol (820  $\text{cm}^{-1}$ ) compared to that between methanol and ethanol (306  $\text{cm}^{-1}$ ). A similar effect is found for the basicity in the series  $\text{NH}_3$ ,  $\text{CH}_3\text{NH}_2$ , and  $\text{CH}_3\text{CH}_2\text{NH}_2$ , where the  $\text{p}K_a$  values are 9.25, 10.64, and 10.67, respectively<sup>28</sup> (note that there could be some solvent hydrogen-bonding effects in these values).

It is important to recognize that only the difference in binding energy from the ionic ground state compared to the neutral ground state is obtained in this work (*i.e.*  $\Delta\text{IE}$ , the lowering of the IE value on complexation), but in the neutral, the total binding energy is much lower. It is assumed that the differences in binding energies in the  $S_0$  and  $S_1$  states are small, and so it is the large changes (electronic and structural) in the ionic states that are dominating the changes in  $\Delta\text{IE}$  by varying the solvent molecule. As well as inductive effects as noted above, there are other factors that can be important in determining the stability of the ion: in the phenol dimer work,<sup>7,29</sup> for example, it was noted that ring-ring interactions could be significant.

**B. The Lack of a "Symmetry Effect".** As noted in the Introduction, one of the reasons why this study was performed was that it was thought that the symmetry of the phenol-water complex was the reason for the large difference between the ZEKE spectra of phenol-water<sup>4</sup> and that of phenol-methanol.<sup>5</sup> In fact, the ZEKE spectrum of phenol-ethanol<sup>6</sup> (contrary to initial thoughts) turned out to resemble that of the phenol-water rather

(26) Dopfer, O.; *et al.* To be submitted.

(27) Hussein, M. A.; Millen, D. J. *J. Chem. Soc., Faraday Trans. 2* 1976, 72, 693.

(28) Sykes, P. *A Guidebook to Mechanism in Organic Chemistry*, 5th Ed.; Longman: New York, 1981; p 65.

(29) Connell, L. L.; Ohline, S. M.; Joireman, P. W.; Corcoran, T. C.; Felker, P. M. *J. Chem. Phys.* 1992, 96, 2585.

than that of phenol-methanol, which already hinted that the story would not be so straightforward.

One reason for the lack of symmetry in the case of the phenol-DME complex might be that the methyl groups are breaking the  $C_s$  symmetry. However, using *ab initio* theory, Cremer *et al.*<sup>30</sup> (HF/4-21G) and very recently Dasgupta *et al.*<sup>25</sup> (HF/6-31G\*\*) have investigated the DME molecule and it was found in both studies that the so-called "double-staggered" rotamer (with equivalent  $\text{CH}_3$  groups and  $C_{2v}$  symmetry) is the most stable conformation, in agreement with experimental results. This would give  $C_s$  symmetry for the complex and so a "symmetry effect" would be expected. Assuming that the  $S_1$  state and the ionic state were also of  $C_s$  symmetry, only the three  $A'$  vibrations would be expected to contribute to the ZEKE spectrum in single quanta; only double quanta of the  $A''$  vibrations would be excited. However, the ZEKE spectra of phenol-DME look like those of phenol-methanol, which is of  $C_1$  symmetry. It thus appears that the idea of a "symmetry effect" in these complexes is redundant. This could be easily explained if the  $S_1$  state was not of  $C_s$  symmetry (*e.g.* if the methyl groups were rotated away from the "double-staggered" conformation), but no data are available to ascertain whether this is true or not. A similar, although less pronounced, effect occurs for phenol-water,<sup>4</sup> where also antisymmetric intermolecular vibrations are believed to have been seen in the ZEKE spectra, despite the fact that the  $S_0$  and ground ionic states are of  $C_s$  symmetry.

## V. Conclusions

The two-color ( $1 + 1'$ ) mass-selected REMPI spectrum of the 1:1 phenol-DME complex has been recorded, and it has been

(30) Cremer, D.; Binkley, J. S.; Pople, J. A.; Hehre, W. A. *J. Am. Chem. Soc.* 1974, 96, 6900.

shown that the interpretation of an earlier LIF study was, in part, erroneous. In particular, the existence of different isomers in the  $S_1$  spectra has been disproved. The origin of the  $S_1 \leftarrow S_0$  transition of the phenol-DME complex has now been identified correctly at  $35\,893.6\text{ cm}^{-1}$ . Intermolecular modes of *ca.* 26.5 and  $141\text{ cm}^{-1}$  were seen, and these were assigned to an intermolecular bend and the intermolecular stretch of the  $S_1$  state of the single isomer. The intermolecular stretch had not been observed previously.

The ZEKE spectra are interpreted in terms of the six intermolecular modes of the cation (albeit tentatively in the case of the  $\eta_4$  vibration). These have frequencies 24, 57, 109, 141 (tentative), 196, and  $275\text{ cm}^{-1}$ , with the latter being assigned to the intermolecular stretch. The large increase of the strength of the hydrogen bond in the cation and the increase in the intermolecular stretch frequency over that in the  $S_1$  state both demonstrate the increased intermolecular forces present in the cation, mainly owing to the additional charge-dipole interaction. The ionization energy was determined accurately as  $62\,604 \pm 5\text{ cm}^{-1}$ . Changes in the lowerings of the ionization energies for the series of phenol-X complexes were interpreted in terms of the positive inductive effects of alkyl groups.<sup>31</sup>

**Acknowledgment.** The authors are grateful to Professor E. W. Schlag (Garching) for his support and encouragement while this work was performed. T.G.W. is grateful for the award of a Royal Society Postdoctoral Fellowship under the European Science Exchange Programme for the time he was at Munich. Financial support for this work from the Deutsche Forschungsgemeinschaft (Grant No. Mu 547/7-1) and the European Community under the Science Program (Grant No. SC1\*-CT90-0642-MD) is gratefully acknowledged.

(31) Müller-Dethlefs, K.; Dopfer, O.; Wright, T. G. *Chem. Rev.*, in press.